Virchows Arch [Pathol Anat] (1986) 409:595–607

Virchows Archiv A

Three-dimensional studies of acellular glomerular basement membranes in dense-deposit disease

Noel Weidner[1], and William B. Lorentz, Jr.[2]
Departments of Pathology[1] and Pediatrics[2], Wake Forest University,
The Bowman Gray School of Medicine, Winston-Salem, NC 27103, USA

Summary. After digestion removed the cells from glomeruli of frozen kidney tissue, we employed scanning electron microscopy to examine the acellular glomerular basement membranes (AGBM) from normal kidneys and from kidneys of patients with dense-deposit disease (DDD). The AGBM showed previously unrecognized three-dimensional patterns of pathologic changes. When compared to normal controls, the AGBM in DDD appeared "rigid" and thickened. Other pathologic features included coarsely granular or undulating epimembranous surfaces punctuated by single or clustered crater-like deformities. Although epimembranous crater-like deformities have been observed in other glomerulopathies, the combination of "rigid"-appearing AGBM punctuated by crater-like deformities is thus far unique to DDD.

Key words: Glomerulonephritis – Membranoproliferative – Scanning electron microscopy – Basement membranes

Introduction

Recently, techniques have been developed allowing removal of the cellular constituents of glomeruli leaving behind the acellular glomerular basement membranes (AGBM) (Carlson and Chatterjee 1983; Carlson and Kenney 1980, 1982). These AGBM preparations can be viewed by scanning electron microscopy (SEM), a technique allowing three-dimensional analysis. The three-dimensional morphologic features of the AGBM can then be correlated with the corresponding features defined by more conventional two-dimensional techniques, such as light microscopy (LM) and transmission electron microscopy (TEM).

Offprint requests to: N. Weidner at the above address

We have previously reported the three-dimensional pathologic changes in AGBM in a series of patients with the various forms of lupus nephritis (Weidner and Lorentz 1986a) and in patients with various stages of idiopathic membranous nephropathy (Weidner and Lorentz 1986b). In a similar fashion, Bonsib (1985a, c) has examined AGBM prepared from selected patients with minimal change disease, idiopathic membranous nephropathy, focal glomerulosclerosis, necrotizing glomerulonephritis, post-infectious glomerulonephritis, and membranoproliferative glomerulonephritis (MPGN) type III. As the basis of this report, we have studied the three-dimensional pathologic changes of the AGBM from patients with dense-deposit disease (DDD) (also known as MPGN type II). We report our findings and correlate them with traditional two-dimensional findings.

Materials and methods

To provide baseline data regarding normal structural variations, normal kidney tissue removed from six patients at autopsy was extracted by the same technique used to extract patient material. The patients ranged in age from 1 month to 71 years (average, 39 years); 4 were males. To eliminate the possibility of freezing-induced artifacts, three of these samples were processed both before and after freezing.

Six renal biopsy samples from five patients with DDD were selected from frozen biopsy fragments remaining after the completion of immunofluorescent studies. The clinical and LM features of these patients are shown in the accompanying table. Biopsy material from all these patients satisfied the diagnostic criteria for DDD as outlined by Sibley and Kim (1984). All the biopsies were obtained by percutaneous needle technique.

The technique for AGBM preparation followed that described by Carlson and coworkers (1980, 1982, 1983) and Bonsib (1984). Thawed renal biopsy fragments were treated consecutively with the following reagents: 1–5 mM EDTA (at least 100:1 vol/vol ratio) at 4° C for 24–72 h, 3% Triton X-100 at room temperature for 8–18 h, 0.025% deoxyribonuclease in 1 M NaCl at room temperature for 2–6 h, and 1–4% sodium deoxycholate at room temperature for 8–18 h. (All chemicals were supplied by Sigma Chemical Co., St. Louis, MO, USA). All solutions contained 0.1% sodium azide, and tissues were washed with large volumes of distilled water between solutions. Washing was especially important after the Triton X-100 and deoxyribonuclease steps. This technique exposed portions of at least two glomeruli per biopsy. In addition, numerous tubular basement membranes were exposed, allowing large expanses of the acellular tubular basement membrane (ATBM) surface to be visualized by SEM. Glomeruli were cross-sectioned to allow visualization of the endothelial AGBM surface.

Extracted tissues were fixed in either 10% formaldehyde or 2% glutaraldehyde, and routine techniques were employed for SEM and TEM. Tissues for SEM were dehydrated in graded alcohols, dried to the critical point, and vacuum-coated with gold-pallidium. Tissues for TEM were cut into 1-mm cubes, postfixed in 1% osmium tetroxide, dehydrated in graded alcohols and propylene oxide, and embedded in Epon. Thin sections were stained with uranyl acetate and lead citrate. SEM was performed with a Philips SEM-501; TEM with a Philips EM-400. Using the Philips SEM-501 "micron-marker" system, we measured the approximate size and density of deformities on the AGBM surfaces. This technique employs a bar calibrated in microns which appears on the screen and is printed within each picture frame. Because of the undulating nature of the AGBM surface, we could only approximate the density of the deformities. This approximation, done on 20 to 30 randomly selected samples per glomerulus, was made by counting the number of deformities in multiple 25-μ^2 samples of AGBM surface. Counting samples in this manner at high magnification tended to "flatten" the AGBM surface and reduce error secondary to surface undulation.

The AGBM and ATBM three-dimensional pathologic findings were correlated with the corresponding two-dimensional findings obtained by conventional LM and TEM techniques.

Results

Controls

SEM examination of AGBM prepared from the healthy kidneys obtained at autopsy revealed smooth epimembranous and endothelial surfaces with only rare, small crater-like deformities ranging from 0.1 to 0.3 μ in diameter (Fig. 1A). These deformities, averaging 1 to 2 per glomerulus, appeared to be more common in older patients. The ATBM and capillary basement membranes were smooth (Fig. 1B). No morphologic differences were found between acellular basement membrane preparations from fresh kidneys and those prepared from previously-frozen tissue. On TEM, kidney tissue prepared by the current technique appeared to be composed exclusively of naked basement membranes and connective tissue fibers (Fig. 1C).

DDD specimens

By LM biopsy specimens 1, 2, and 3 displayed diffuse MPGN with "lobular" accentuation of the glomerular segments (i.e., "lobular" glomerulonephritis). Biopsies 4 and 5 displayed focal to diffuse mesangial proliferation with focal-segmental peripheral capillary loop thickening (see Table). Renal tubules, interstitium, and vessels appeared normal by LM in all biopsies.

On SEM the configuration of the AGBM in biopsies 1, 2, 4, and to a lesser extent in 3, suggested thickened AGBM that was "rigid" or fixed (Fig. 2A). Indeed, where viewed in cross-section, the AGBM was thickened relative to normal control AGBM. In biopsies 1, 2, and 4 the epimembranous AGBM surfaces were coarsely granular and punctuated by crater-like deformities (Figs. 2A, 2B and 3A). On TEM the coarsely granular surfaces corresponded to irregularly thickened AGBM containing dense intramembranous deposits (Figs. 2C, 2D and 3B, 3C). The crater-like deformities corresponded to extensions of GBM along the epimembranous surfaces. The latter were often adjacent to epimembranous electron-dense deposits (EDDs) that were extracted during the cellular digestion process (Figs. 2D and 3C). On SEM of biopsy 3 the epimembranous AGBM surfaces were smooth to finely-granular, forming folded and undulating segments (Fig. 4A). Crater-like deformities were occasionally present (Fig. 4A, inset). On TEM of biopsy 3 the folded and undulating AGBM segments corresponded to undulating GBM containing dense intramembranous deposits (Fig. 4B). Like previous biopsies, the crater-like deformities likely corresponded to extensions of GBM found around epimembranous electron-dense deposits (Fig. 4B, inset). SEM of biopsies 5a and 5b revealed epimembranous AGBM surfaces that were smooth to finely granular; and, in contrast to previous cases, the AGBM did not appear thickened and "rigid". Occasional segmental clusters of crater-like deformities were present.

In biopsy 1 the crater-like deformities were "ring"-shaped, single, and infrequently distributed over the epimembranous AGBM surfaces (4 to 5 per glomerulus). They averaged 0.3 μ in greatest diameter. In biopsy 2 the

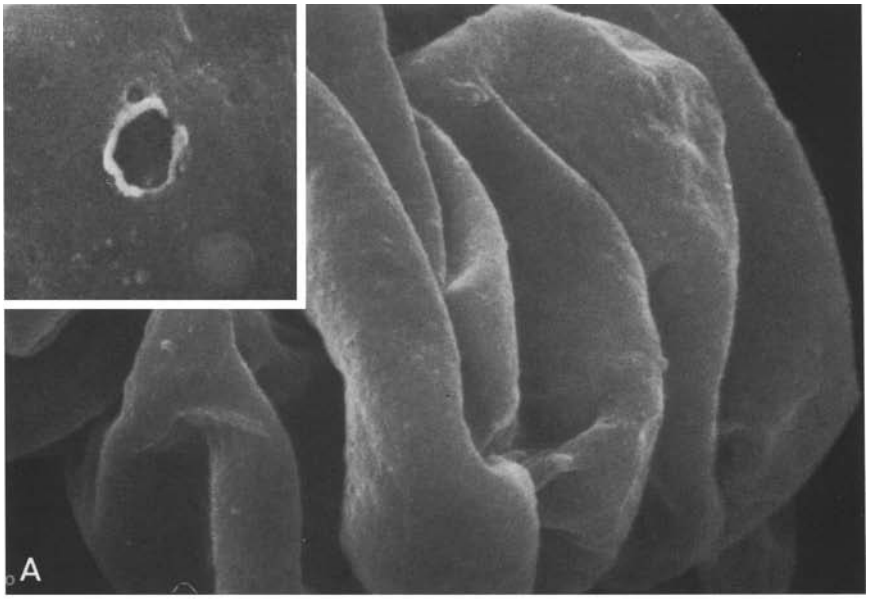
A


B

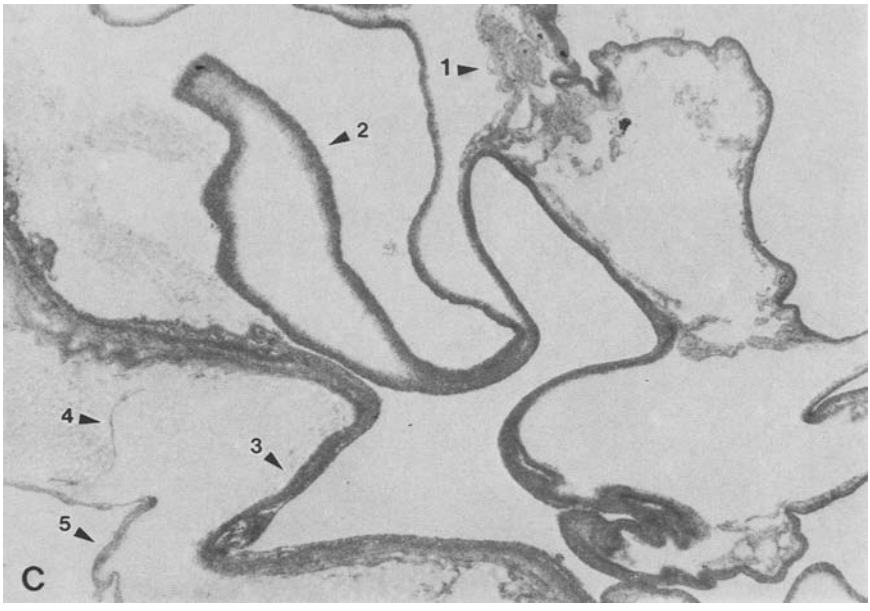

Fig. 1. A *(normal autopsy kidney)*. SEM view of the AGBM showing the smooth epimembranous surface (Original magnification, ×2,500). Inset shows in greater detail a 0.3 μ diameter crater-like deformity, occasionally found on the epimembranous acellular glomerular basement membrane surface (Original magnification ×20,000). **B** *(normal autopsy kidney)*. SEM view of the renal parenchyma showing smooth epithelial ATBM surface with interstitial connective tissue fibers and capillary basement membranes (*arrows*) (Original magnification ×1,250). **C** *(normal autopsy kidney)*. TEM view of acellular basement membrane preparation (Original magnification ×2,500). All cellular material has been extracted leaving basement membrane and connective tissue. The numbered arrows (1 thru 5) point to mesangium, acellular glomerular basement membrane, Bowman's membrane, acellular tubular basement membrane, and connective tissue fibers, respectively

crater-like deformities occurred alone and in segmental clusters. Some were "ring"-shaped, but more frequently they formed confluent groups of reticulated crater-like deformities (Fig. 2B). In biopsy 2 they ranged in size from 0.1 to 0.8 μ in greatest diameter, averaging 0.3 μ; there were approximately 800 crater-like deformities per 1,000 μ^2 of AGBM surface. In biopsy 3 "ring-shaped" crater-like deformities were rare (4 to 5 per glomerulus), averaging 0.8 μ in greatest diameter (Fig. 4A, inset). In biopsy 4 there were approximately 250 crater-like deformities per 1,000 μ^2 AGBM, and they ranged in greatest diameter from 0.1 to 0.4 μ, averaging 0.2 μ. In biopsy 5 the clustered crater-like deformities were rare (3 to 4 per glomerulus) and ranged in greatest diameter from 0.1 to 0.8 μ, averaging 0.5 μ.

In all biopsies epimembranous immune-complex-like deposits were extracted by the cellular digestion technique. Dense intramembranous deposits appeared less dense by TEM in extracted AGBM when the latter was compared to GBM of the same biopsy prior to extraction (Fig. 3C). On SEM

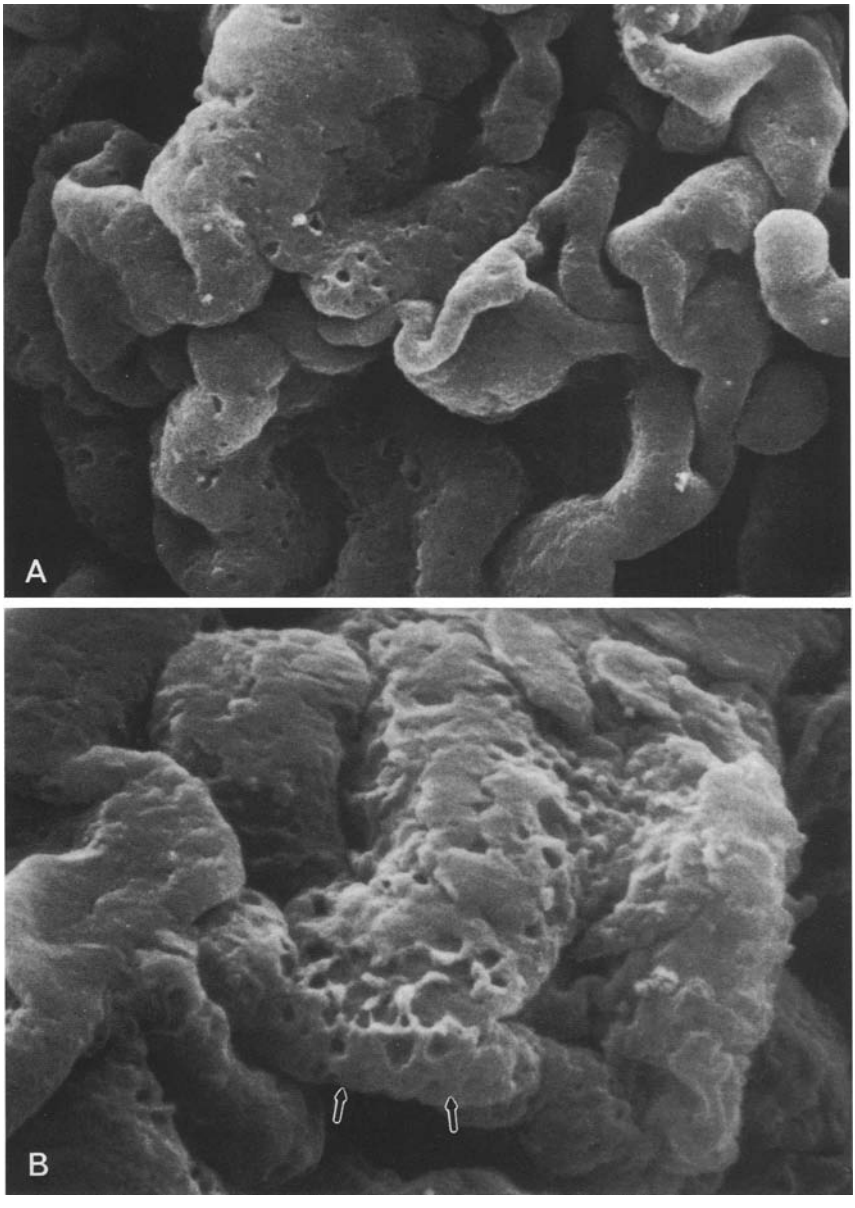

Fig. 2. A *(biopsy # 2)*. SEM view of AGBM in a patient with dense-deposit disease. Note the "rigid" configuration of the loops of AGBM which are also segmentally punctuated by crater-like deformities (Original magnification ×1,250). **B** *(biopsy # 2)*. SEM view of AGBM showing a confluent and reticulated cluster of crater-like deformities (*arrows*) (Original magnification ×5,000). **C** *(biopsy # 2)*. TEM view of multiple glomerular segments before cellular extraction. Note segment of glomerular basement membrane (*open arrows*) containing dense

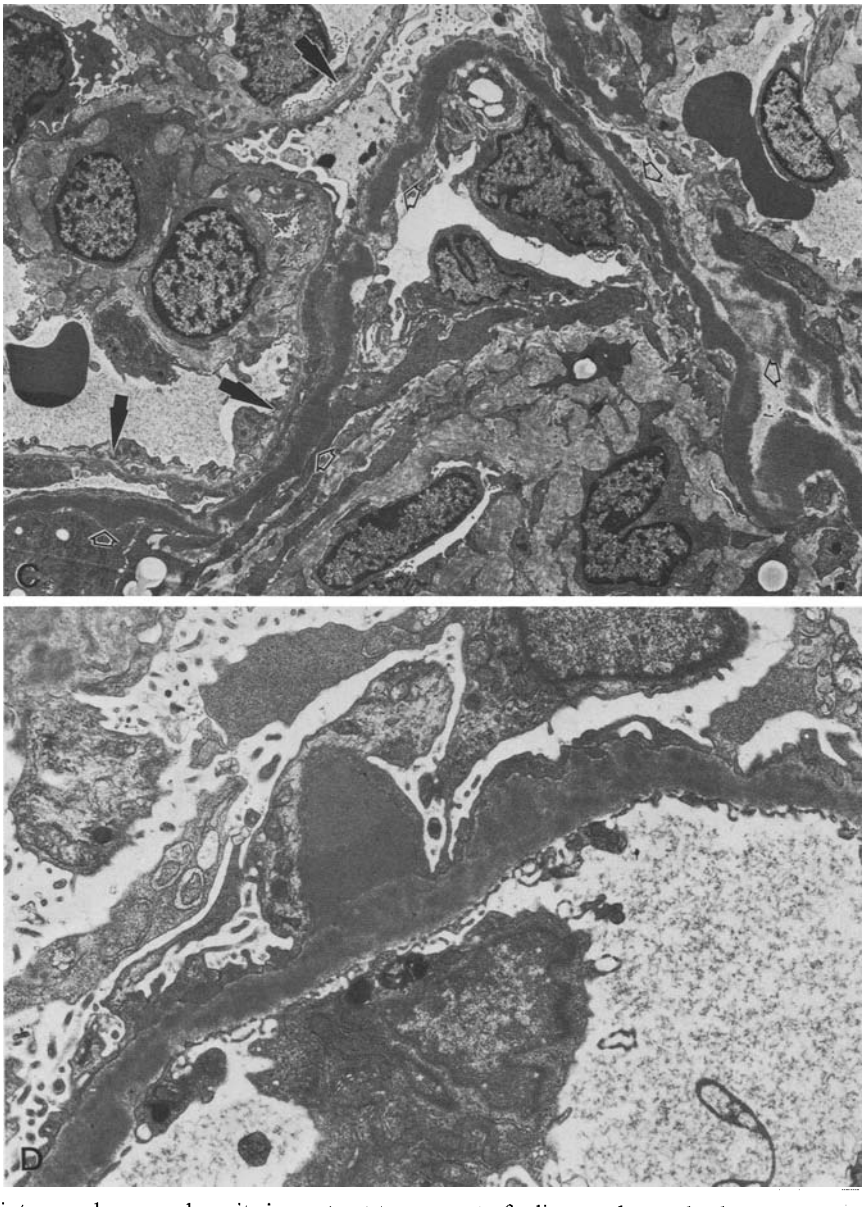

intramembranous deposits in contrast to segment of adjacent glomerular basement membrane (*closed arrows*) without dense intramembranous deposits (Original magnification ×1,990). **D** *(biopsy # 2)*. TEM view of a glomerular segment at higher magnification before cellular extraction. Note dense intramembranous deposits, irregularly thickened basement membrane, and "hump-like" electron-dense deposit (Original magnification ×15,000)

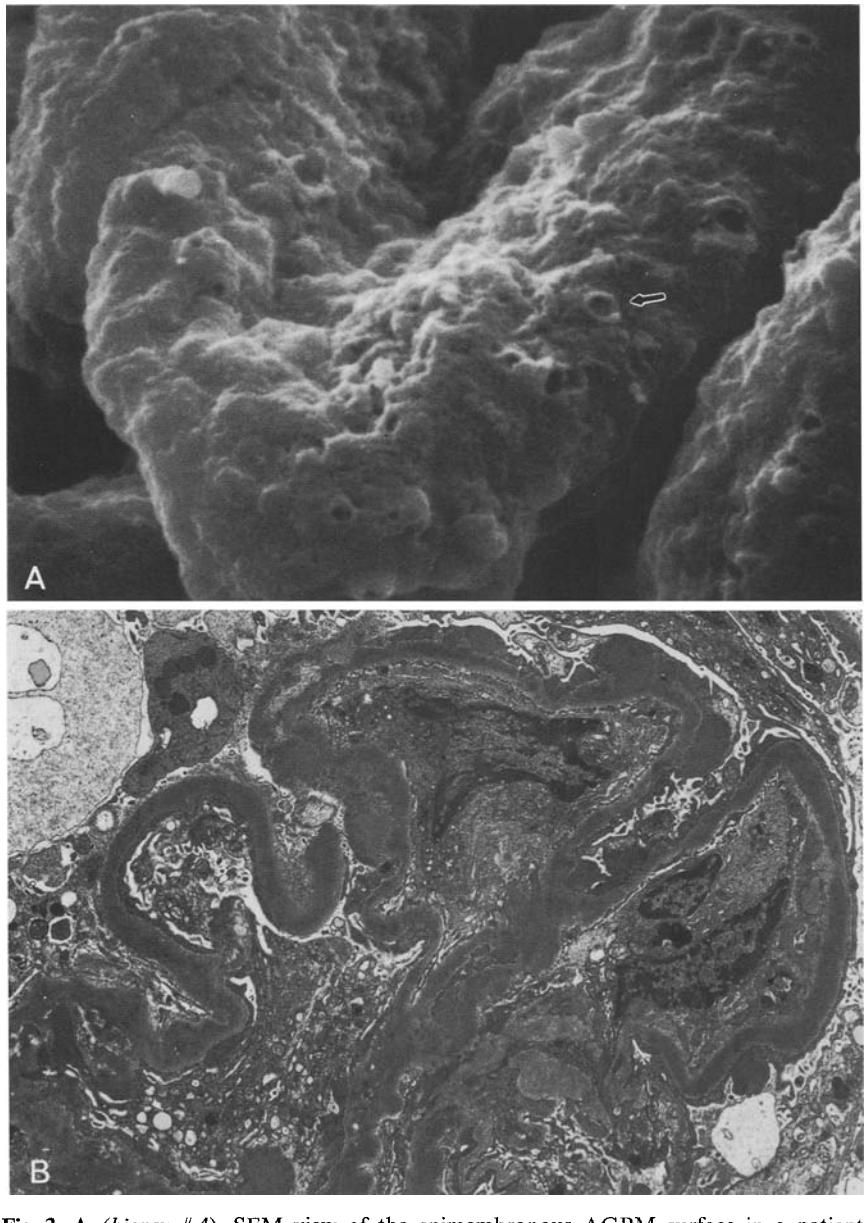

Fig. 3. A *(biopsy # 4)*. SEM view of the epimembranous AGBM surface in a patient with DDD showing course granularity and scattered "ring-shaped" crater-like deformities (*arrow*) (Original magnification ×10,000). **B** *(biopsy # 4)*. TEM view of multiple glomerular segments before cellular extraction. Note extensive incorporation of confluent dense deposits within the lamina densa of the glomerular basement membrane (Original magnification ×3,300). **C** *(biopsy # 4)*. TEM view of a glomerular segment at higher magnification showing irregularly thickened glomerular basement membrane containing dense intramembranous deposits, epimembranous EDDs, and perideposit epimembranous extensions of basement membrane (Original magnification ×15,000). Inset shows TEM view of a dense intramembranous deposit after cellular extraction. It appears less dense than before extraction suggesting partial extraction. All epimembranous EDDs have been extracted (Original magnification ×20,000)

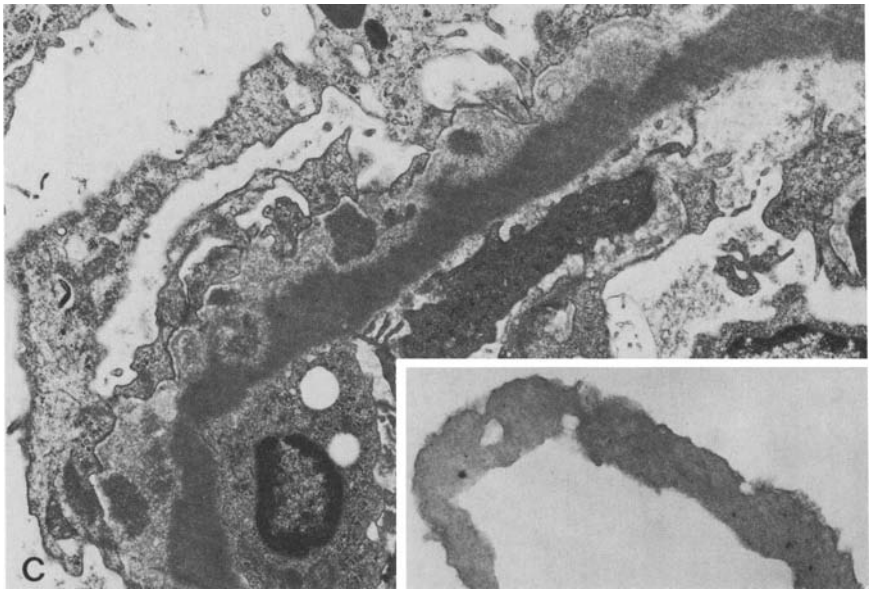

the endothelial GBM surfaces and ATBM surfaces were smooth in all biopsies.

Discussion

When the current extraction technique is applied to diseased renal glomeruli, previously unrecognized patterns of pathologic change can be viewed. Thus far, AGBM from a variety of glomerulopathies have been studied by SEM. These include lupus nephritis (Weidner and Lorentz 1986a), idiopathic membranous nephropathy (Weidner and Lorentz 1986b; Bonsib 1985a), minimal-change disease (Bonsib 1985a), focal glomerulosclerosis (Bonsib 1985a), necrotizing glomerulonephritis (Bonsib 1985b), postinfectious glomerulonephritis (Bonsib 1985c), and MPGN type III (Bonsib 1985c).

In lupus nephritis we observed epimembranous crater-like deformities with and without material resembling immune complexes; severely distorted, "moth-eaten" glomerular basement membrane; and the formation of secondary basement membrane within glomerular capillaries (Weidner and Lorentz 1985a). These three-dimensional changes correlated well with the subclasses of lupus nephritis as defined by the World Health Organization. In idiopathic membranous nephritis, we observed crater-like deformities of the epimembranous AGBM surface that usually formed reticulated and confluent structures (Weidner and Lorentz 1985b). Where EDDs had been incorporated into the GBM, plaque-like areas without crater-like deformities were apparent by SEM. These patterns correlated with stages of membranous nephropathy as defined by Ehrenreich and Churg (1968).

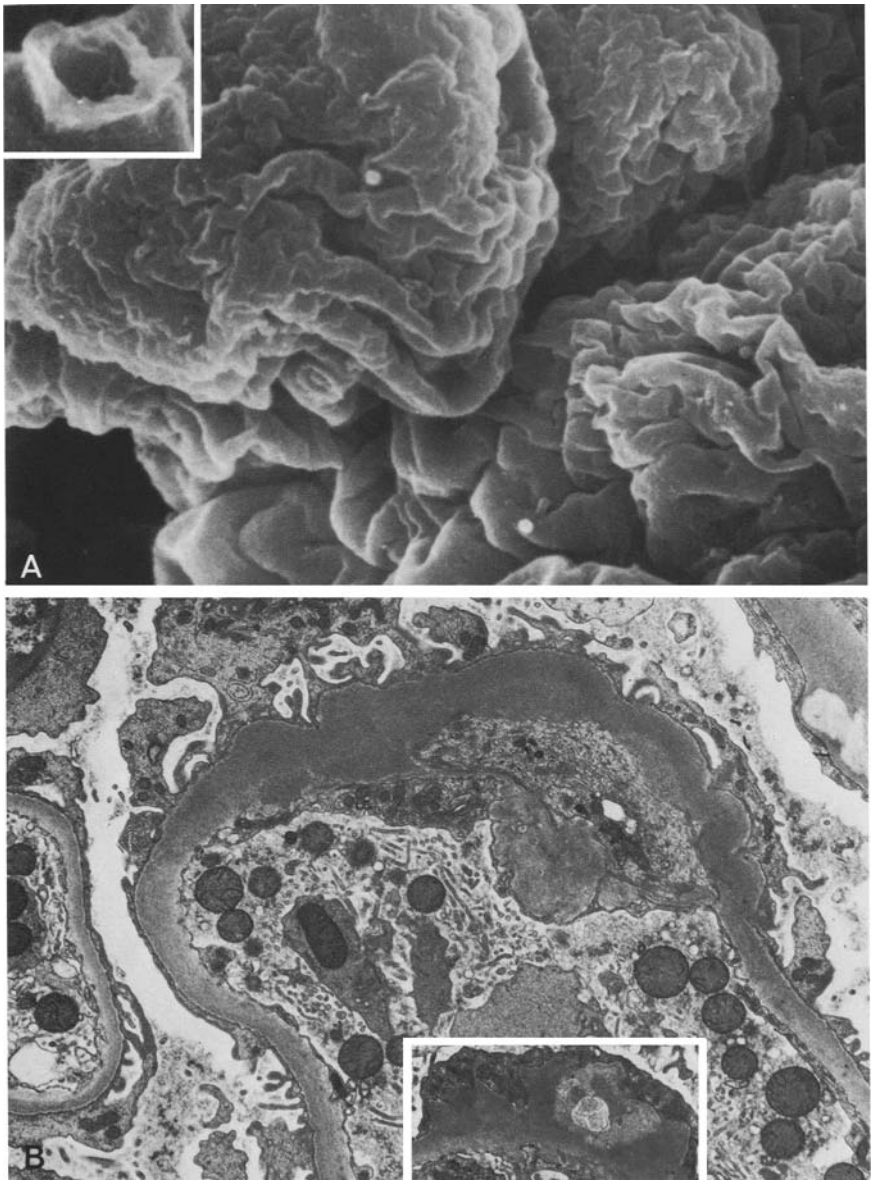

Fig. 4. A *(biopsy # 3)*. SEM view of the epimembranous AGBM surface in a patient with DDD showing smooth surface "thrown" into undulating folded segments (Original magnification ×5,000). Inset shows details of an occasional "ring-shaped" crater-like deformity found in this case (Original magnification ×20,000). **B** *(biopsy # 3)*. TEM view of a glomerular segment before extraction. Note peripheral basement membrane "thrown" into undulating folds and containing dense intramembranous deposits (Original magnification ×15,000). Inset shows TEM view of a crater-like deformity before cellular extraction. The "walls" of the crater-like deformities apparent on the AGBM epimembranous surfaces (see inset, Fig. 4A) likely correspond to extensions of GBM around electron-dense deposits (Original magnification ×11,700)

Table 1. Clinical and laboratory features of the patients with dense-deposit disease

Biopsy #	Age/ sex	Clinical presentation	Urine protein per 24 h (grams)	Creatinine clearance ml/min/m^2	LM findings	Treatment	Follow-up years	Outcome
1.	9/F	NS, decr. C3	5.2	18	MPGN, "lobular" GN	Dipyrid., ASA	5	ESRD in 1.5 years
2.	8/F	NS, decr. C3	2.9	22	MPGN, "lobular" GN	Steroids (alternate day), dipyrid., ASA	3	Persistent proteinuria, SRF
3.	12/M	Proteinuria, decr. C3	9.0	70	MPGN, "lobular" GN	Dipyrid., ASA	0.3	Persistent proteinuria, SRF
4.	6/M	Proteinuria, hematuria, decr. C3	5.4	53	Mesangial prol. GN	Dipyrid., ASA	1	Persistent proteinuria and hematuria, SRF
5A.	8/F	Proteinuria, hematuria, decr. C3	0.8	70	Mesangial prol. GN	Dipyrid., ASA	NA	NA
5B.	9/F	Proteinuria, hematuria, decr. C3	0.2	70	Mesangial prol. GN	Dipyrid., ASA	1.5	Persistent proteinuria and hematuria, SRF

NS = nephrotic syndrome; decr. = decreased; C3 = serum C3; LM = light microscopy; GN = glomerulonephritis; MPGN = membranoproliferative GN; prol. = proliferative; dipyrid. = dipyridamole; ASA = acetosalicyclic acid; NA = not applicable; ESRD = end-stage renal disease; SRF = stable renal function

In a similar fashion, Bonsib has reported the epimembranous AGBM surface to be smooth in minimal change disease and focal segmental sclerosis (Bonsib 1985a). He showed AGBM "gaps" in focal necrotizing glomerulonephritis with crescents (Bonsib 1985b) and illustrated focal-segmental crater-like deformities in MPGN type III, postinfectious glomerulonephritis, and segmental membranous nephropathy (Bonsib 1985c).

When we applied the extraction technique to renal biopsies from patients with DDD, some interesting three-dimensional patterns became apparent. On SEM the overall pattern of the AGBM appeared abnormally "rigid" and thickened (an impression confirmed where cross-sectioned AGBM was available for viewing). The epimembranous AGBM surfaces were coarsely granular or segmentally undulating and punctuated by variable numbers of crater-like deformities. The irregularities apparent on SEM corresponded to areas of GBM containing dense intramembranous deposits, visible by TEM. The rims of the crater-like deformities likely corresponded to GBM elaborated adjacent to EDDs, present before extraction. Although the irregular epimembranous surfaces and crater-like deformities are not unlike similar structures reported in other glomerulopathies, the "rigid" configuration of the AGBM punctuated by crater-like deformities appears thus far unique to DDD. However, this particular combination of three-dimensional abnormalities was not apparent in all cases of DDD. It was best developed in those cases showing numerous dense intramembranous deposits and irregularly-thickened GBM by TEM.

In all the DDD biopsies of this study, the epimembranous EDDs were extracted by the cellular digestion technique. In addition, when dense intramembranous deposits were compared before and after extraction, they appeared less dense; and, therefore, partially extracted. With the exception of some cases of membranous lupus nephritis, EDDs have been uniformly extracted in immune-complex-mediated glomerulonephritis. The reasons for the variable extractability of immune complexes in lupus nephritis remains unknown. However, it is tempting to speculate that deoxyribonucleic acid (DNA)-containing immune complexes (as found in lupus nephritis) have greater affinity for GBM. DNA has, in fact, been shown to have high affinity for the GBM (Izui et al. 1976).

In summary, we present the three-dimensional pathologic features of the AGBM in DDD and compare them to identical studies performed on the AGBM in other glomerulopathies. The extraction technique employed in this study is inexpensive and easy to perform (Weidner and Lorentz 1986a; 1986b). It can be applied to other types or nephritis, and we believe it has potential for yielding additional clinicopathologic information, as well as basic data regarding the biochemistry and immunopathology of kidney basement membrane. It can be easily applied to the three-dimensional evaluation of glomerulonephritis in animal models, and may eventually prove useful as a diagnostic and prognostic tool in selected human glomerulonephritides.

References

Bonsib SM (1984) Scanning electron microscopy of acellular glomeruli in human glomerulonephritis: Application of a technique. Ultrastruct Pathol 7:215–217

Bonsib SM (1985a) Scanning electron microscopy of acellular glomeruli in nephrotic syndrome. Kidney Int 27:678–684

Bonsib SM (1985b) Glomerular basement membrane discontinuities. Scanning electron microscopic study of acellular glomeruli. Am J Pathol 119:357–360

Bonsib SM (1985c) Segmental subepithelial deposits in primary glomerulonephritis: Scanning electron microscopic examination of acellular glomeruli. Hum Pathol 16:1115–1121

Carlson ED, Kenney MC (1980) Preparation and histoarchitecture of ultrastructurally pure glomerular basement membrane. Renal Physiol 3:280–287

Carlson ED, Kenney MC (1982) An ultrastructural analysis of isolated basement membranes in the acellular renal cortex: A comparative study of human and laboratory animals. J Morphol 171:195–211

Carlson ED, Chatterjee SN (1983) Ultrastructure of isolated basement membranes in the acellular human renal cortex. Renal Physiol 6:197–208

Ehrenreich T, Churg J (1968) Pathology of membranous nephropathy. In: Sommers SC (ed) Pathology annual. Appleton-Century-Crofts, New York, p 145

Izui S, Lambert PH, Miescher PA (1976) In vitro demonstration of a particular affinity of glomerular basement membrane and collagen for DNA. A possible basis for local formation of DNA-anti-DNA complexes in systemic lupus erythematosus. J Exp Med 144:428–436

Sibley RK, Kim Y (1984) Dense intramembranous deposit disease: New pathologic features. Kidney Int 25:660–670

Weidner N, Lorentz WB (1986a) Scanning electron microscopy of the acellular glomerular and tubular basement membranes in lupus nephritis. Am J Clin Pathol 85:135–145

Weidner N, Lorentz WB (1986b) Scanning electron microscopy of the acellular glomerular basement membranes in idiopathic membranous nephropathy. Lab Invest 54:84–92

Accepted April 30, 1986